

Electrical properties of $\text{NiS}_{2-x}\text{Se}_x$

P. Kwizera,* M. S. Dresselhaus,[†] and D. Adler[†]

Center for Materials Science and Engineering, Massachusetts Institute of Technology, Cambridge, Massachusetts 02139

(Received 7 May 1979)

We report results of measurements of electrical conductivity, thermoelectric power, and Hall effect on single crystals of $\text{NiS}_{2-x}\text{Se}_x$ ($0.1 \leq x \leq 1.5$). These results cannot be understood using the one-electron approximation but are explained quantitatively by assuming both strong electronic correlations and strong electron-phonon interactions in the $3d e_g$ band associated with the nickel ions. The $\text{NiS}_{2-x}\text{Se}_x$ compounds are of particular interest insofar as they permit study of the effect of increasing bandwidth without a change of the basic occupation of states in the correlation-split e_g bands. In our model, pure stoichiometric $\text{NiS}_{2-x}\text{Se}_x$ ($x < 0.6$) is a Mott insulator with an energy gap due to the correlation splitting of the nickel e_g band. However, in all real samples, nonstoichiometry and/or traces of impurities lead to a small concentration of free carriers at all temperatures. These carriers form small polarons, which ordinarily conduct only by means of thermally activated hopping in a very narrow band. For $0.45 \leq x < 0.6$, the conductivity decreases with increasing temperature below about 100 K. We interpret this unusual behavior as due to small-polaron band conduction, a phenomenon predicted by Holstein and others at low temperatures but heretofore unconfirmed. For $x \geq 0.6$, small polarons do not form, and the system is metallic at all temperatures.

I. INTRODUCTION

For the last decade the pyrite transition-metal dichalcogenides have been intensively studied. Since the pioneering work of Bither,¹ various attempts have been made to understand the electronic properties of these materials.²⁻¹⁰ At present the electronic properties of these materials are thought to be controlled by the properties of the $3d e_g$ band of the transition-metal cations.

The $3d e_g$ band contains four states per cation, so that FeS_2 has an empty e_g band, ZnS_2 has a completely filled e_g band whereas CoS_2 and CuS_2 have one-quarter and three-quarter filled e_g bands, respectively.⁷ The insulating or metallic properties of these compounds are for the most part as predicted above by the e_g band filling; FeS_2 and ZnS_2 are insulators and CoS_2 and CuS_2 metallic. On this scheme, nickel disulfide should have a half-filled band, but it turns out to be semiconducting. To explain the apparently anomalous behavior of NiS_2 it was suggested that NiS_2 is a Mott insulator due to electron-electron correlations in the e_g band.^{1,7,8} It has been recently demonstrated^{11,12} that the Mott-insulator picture does indeed account for the transport properties of NiS_2 .

By alloying NiS_2 with CoS_2 forming solid alloys of the form $\text{Ni}_{1-y}\text{Co}_y\text{S}_2$ it is possible to study the evolution of this system from a semiconductor to a metal.⁷ Recently, results of systematic measurements of several transport properties of $\text{Ni}_{1-y}\text{Co}_y\text{S}_2$ have been reported.^{11,12} A theoretical model that depends on both strong electronic correlations and electron-phonon coupling has been used to interpret the conductivity and thermoelectric power data quantitatively for these materials,

explaining anomalies in the observed behavior.

In this paper we report the corresponding transport properties of the alloy system $\text{NiS}_{2-x}\text{Se}_x$. NiSe_2 is metallic in agreement with arguments based on the filling of the $3d e_g$ band so that increased selenium concentration must eventually yield a semiconductor-metal transition. Such a transition was observed in the $\text{Ni}_{1-y}\text{Co}_y\text{S}_2$ system,^{7,11} but in that case the alloying introduced holes in the valence band. In the $\text{NiS}_{2-x}\text{Se}_x$ system, the alloying simply increases the bandwidth without changing the carrier concentration. The data on the $\text{Ni}_{1-y}\text{Co}_y\text{S}_2$ system could be explained only by the assumption that the effective electronic bandwidth in the $3d e_g$ band is extremely narrow.¹¹ This assumption provided a fit to the data for temperatures in excess of about 100 K. Such narrow bandwidths require the existence of small polarons, and, in fact, small polaron hopping was found to dominate the transport even after the correlation-induced gap collapsed.¹¹ In this regard, introduction of Se in place of S is extremely interesting, since the increased bandwidth should lead to a breakdown of the previous theory at higher temperature.⁷

Conductivity measurements have previously been reported¹³ for the $\text{NiS}_{2-x}\text{Se}_x$ system for $0 < T \leq 300$ K. In this work, we extend these measurements to 600 K and provide a quantitative fit for the data in the semiconducting regime. We also report the results of thermoelectric power measurements over the same temperature range and fit the data in the semiconducting region using the same model. For $0.4 \leq x < 0.6$, at very low temperature, $50 \leq T \leq 150$ K, we identify the predominant transport mechanism as conduction in a

small-polaron band.¹⁴ In this regime, the electrical conductivity decreases with increasing temperature due to a decrease in bandwidth, much as originally was predicted by Holstein.¹⁴ Finally, we present some general discussion on the connection between this interpretation of the $\text{NiS}_{2-x}\text{Se}_x$ transport properties and recent attempts to understand the electronic properties of NiS_2 .^{7,11,12}

II. EXPERIMENTAL DETAILS

The experimental procedures used in this work are similar to those used by Mabatah *et al.*¹¹ and are described more fully elsewhere.¹⁵ Single crystals of $\text{NiS}_{2-x}\text{Se}_x$ were grown by chemical vapor deposition in a manner similar to previous work,¹³ except that bromine rather than chlorine was used as the transport agent. Stoichiometric mixtures of pure nickel, sulfur, and selenium were used to prepare a polycrystalline starting material, from which single crystals were grown. The sulfur and nickel were "Specpure" powders from Johnson Matthey chemicals, and were pure to within a few parts per million. The selenium used was selenium shot (99.99%) from Ventron Alfa Products. The samples were characterized by x-ray lattice constant measurements, utilizing the observed linear increase in lattice constant with increasing Se concentration x .¹⁶ (We denote by x and x^* respectively the nominal Se concentration and that determined by lattice constant measurements using Ref. 16.) The lattice constant measurements were made on back reflection for 2θ in the range $120 \leq 2\theta \leq 165^\circ$ using a powder Norelco diffractometer. All our samples for $0.1 \leq x \leq 0.8$ were found to be stoichiometric to within 5% except for the $x = 1.5$ sample, which was selenium deficient by ~15%. This selenium deficiency is probably due to the ~10% sulfur excess used in the crystal growth process as required by the phase diagram for the disulfide formation. Table I gives the values for x and x^* for the samples used in the present study.

Conductivity measurements were made for the temperature range $4 \leq T \leq 600$ K using a 4-probe van der Pauw technique¹⁷ and Hall mobility measurements for six $\text{NiS}_{2-x}\text{Se}_x$ samples in the range $0.1 \leq x \leq 0.8$ for the temperature range $80 \leq T \leq 300$ K and the magnetic field range $0 \leq B \leq 15$ kG. Thermopower measurements were made in the range $80 \leq T \leq 600$ K using the heat pulse technique.¹⁸

III. RESULTS

A. Electrical conductivity

The results of the conductivity measurements for $\text{NiS}_{2-x}\text{Se}_x$ $0.1 \leq x \leq 1.5$ shown in Fig. 1 indicate

TABLE I. Lattice constant a_0 for various nominal selenium concentrations x of the $\text{NiS}_{2-x}\text{Se}_x$ system.

Nominal selenium concentration x	$x^*{}^a$	a_0 (Å)
0 ^b		5.6874
0.1	0.10	5.7020
0.2	0.20	5.7170
0.3	0.29	5.7206
0.4	0.40	5.7463
0.52	0.51	5.7589
0.55	0.54	5.7616
0.8	0.77	5.7770
1.5	1.20	5.8410
2.0 ^b		5.9604

^a x^* is Se concentration determined from x-ray measurements.

^bThe results for NiS_2 and NiSe_2 , i.e., $x = 0$ and $x = 2.0$ are taken from Ref. 1.

thermally activated behavior for $x \leq 0.55$ and tend to a common maximum of $\sim 10^3 \Omega^{-1} \text{cm}^{-1}$ at high temperatures. The results for $x \leq 0.55$ are qualitatively similar to those for pure NiS_2 and for $\text{Ni}_{1-y}\text{Co}_y\text{S}_2$ with $y \leq 0.05$. These data show three distinct activation energies (see Fig. 2). These activation energies all decrease with increasing x , and approach zero as x approaches 0.6 (see Fig. 3), the Se concentration at which the insulator-to-metal transition occurs. For higher x , the samples are metallic over the entire range of temperature $4 \leq T \leq 600$ K. Samples with low

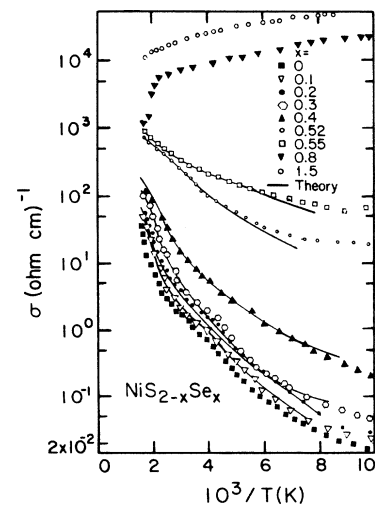


FIG. 1. Conductivity versus inverse temperature. The experimental data are shown using the symbols of the legend. The solid lines are the theoretical fits made for the semiconducting regime $x \leq 0.55$. The data for NiS_2 are taken from Ref. 11.

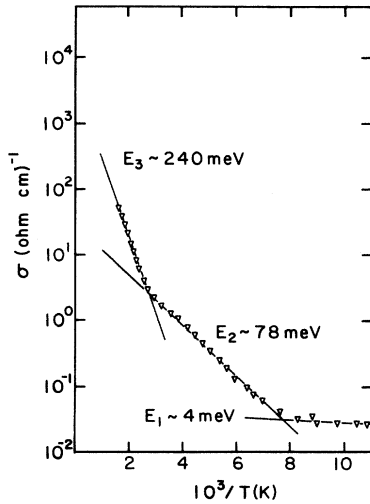


FIG. 2. Conductivity versus inverse temperature for $\text{NiS}_{1.9}\text{Se}_{0.1}$. The three activation energies E_1 , E_2 , and E_3 are obtained from the slopes of the lines shown in the figure.

selenium concentrations, $x \leq 0.3$, have at all temperatures a conductivity behavior similar to pure NiS_2 and to $\text{Ni}_{1-y}\text{Co}_y\text{S}_2$ for $y \leq 0.05$; on the other hand, the three samples in the range $0.4 \leq x \leq 0.55$ exhibit a transition at low temperatures ($T \leq 100$ K) to a metalliclike state as shown in Fig. 4. This is in agreement with Bouchard *et al.*¹³ who also reported this low-temperature quasimetallic phase that does not occur in pure NiS_2 . Bouchard *et al.*¹³ have carried out an intensive study of the

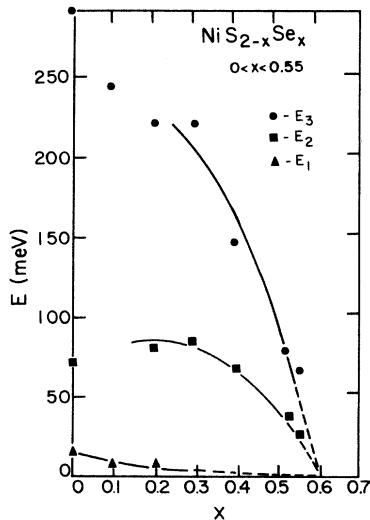


FIG. 3. Activation energies E_1 , E_2 , and E_3 vs selenium concentration x . E_1 corresponds to low temperature, E_2 to intermediate temperature, and E_3 to high temperature (see Fig. 2). All the activation energies E_1 approach (broken curves) zero for $x \sim 0.6$ at the metal-insulator transition.

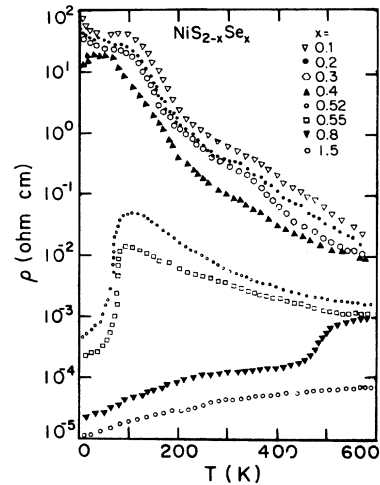


FIG. 4. Resistivity versus temperature for the same data as in Fig. 1 but giving emphasis to the low-temperature behavior. These data compare well with results in Ref. 13 for $T \leq 300$ K, the temperature range of that reference.

conductivity of the $\text{NiS}_{2-x}\text{Se}_x$ system. In our work, we focus our attention mainly on the behavior of this system in the semiconducting regime. Our results are in general agreement with those of Bouchard *et al.*¹³ with regard both to the values of x for which the semiconductor-to-metal transition exists and to the low-temperature ($T \leq 100$ K) behavior of compounds with $0.4 \leq x \leq 0.55$.

B. Hall effect

Hall-effect data could prove to be extremely useful in understanding the transport mechanisms in the $\text{Ni}_{2-x}\text{Se}_x$ system. However, the Hall signal was too small to detect with our equipment over the temperature range $80 \leq T \leq 300$ K and magnetic field range $0 \leq B \leq 15$ kG; thus, only an upper bound of $\mu_H \leq 0.8$ $\text{cm}^2/\text{V-sec}$ can be given for the Hall mobility.

C. Thermoelectric power

Figure 5 shows the results for the thermoelectric power as a function of temperature for various Se concentrations with $x \leq 0.55$. For this range of Se concentrations, the thermopower is small and approximately temperature independent above a "saturation temperature" T_s at which point S approaches its high-temperature limit S_∞ . It is clear from Fig. 5 that T_s decreases with increasing x . The saturation value of the thermopower S_∞ tends to a constant value ($S_\infty \approx -30$ $\mu\text{V}/\text{K}$), independent of x , in the saturation regime $T > T_s$ for $0.2 \leq x \leq 0.55$. Other characteristic temperatures such as the thermopower peak tem-

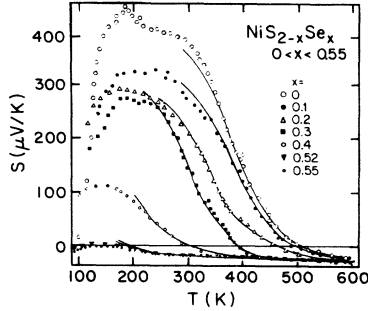


FIG. 5. Thermoelectric power versus temperature. The experimental data are for various Se concentrations (see symbol legend) and the solid curves represent the theoretical fit. The NiS_2 data are taken from Ref. 11.

perature T_p (where S is a maximum S_p) and the crossover temperature T_0 (where S changes sign) are also decreasing functions of the Se concentration x . A summary of the dependence of the critical parameters on Se concentration is given in Table II. The temperature dependence of the thermopower for $x \leq 0.55$ is qualitatively the same as in the $\text{Ni}_{1-y}\text{Co}_y\text{S}_2$ system in the range $0 \leq y \leq 0.12$.¹¹ Also the y dependence of the S_p , T_0 , T_p , T_s parameters in the $\text{Ni}_{1-y}\text{Co}_y\text{S}_2$ system is very similar to their x dependence in the $\text{NiS}_{2-x}\text{Se}_x$ system.¹¹ The saturation value S_∞ for the two systems also has approximately the same magnitude with $S_\infty = -30 \mu\text{V/K}$ for the $\text{NiS}_{2-x}\text{Se}_x$ system and $S_\infty = -38 \mu\text{V/K}$ for the $\text{Ni}_{1-y}\text{Co}_y\text{S}_2$ system.

For $x = 0.8$, which is metallic for the entire temperature range $4 \leq T \leq 600$ K, the thermopower decreases linearly with temperature as expected (see Fig. 6).

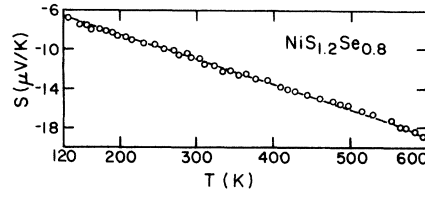


FIG. 6. Thermoelectric power versus temperature for $\text{NiS}_{1.2}\text{Se}_{0.8}$. The data are shown by circles and the line is passed through the experimental points.

IV. DISCUSSION

A. Semiconducting region

The main features of a theoretical model that accounts for the electrical conductivity and thermopower for the $\text{Ni}_{1-y}\text{Co}_y\text{S}_2$ system have been reported elsewhere.^{7,11,12} In this section we show that this model is also capable of explaining the transport properties of the $\text{NiS}_{2-x}\text{Se}_x$ system. According to the model, the $3d e_g$ band is split by strong electronic correlations with a resulting energy gap $E_g = U - \Delta$, where U is the intraionic Coulomb repulsion and Δ is the bandwidth. In pure NiS_2 , the lower band is full and the upper band is empty, so that NiS_2 is a semiconductor. Hall measurements indicate that transport can be associated with carriers having large effective masses, thereby suggesting the formation of small polarons.¹⁴ If small polarons form, we can expect that $\Delta \ll U$, so that $E_g \approx U$. The temperature dependence of the energy gap is then given by $U(T) = U_0 - \gamma kT$, where U_0 is the value of U at $T = 0$ and γ is a constant.¹⁹ This allows us to distinguish

TABLE II. Values for various thermopower parameters for $\text{NiS}_{2-x}\text{Se}_x$, $0 \leq x \leq 0.55$.

Selenium concentration x	T_0^a (K)	S_p^b ($\mu\text{V/K}$)	T_p^c (K)	S_{600}^d ($\mu\text{V/K}$)	T_s^e (K)
0	500	450	230	-6	NA (> 600)
0.1	480	330	225	-23	NA (> 600)
0.2	455	287	200	-29	550
0.3	387	275	187	-29	475
0.4	295	113	145	-28	400
0.52	138	0	138	-29	400
0.55	138	0	138	-29	400

^a T_0 is the crossover temperature, i.e., temperature where the thermopower vanishes.

^b S_p is the peak or maximum thermopower.

^c T_p is the temperature at which a peak thermopower occurs.

^d S_{600} is the thermopower at 600 K, which for $x > 0.1$ is equivalent to S_∞ .

^e T_s is the temperature at which the thermopower becomes temperature independent.

For the available temperature range, T_s is not observed for $x \leq 0.1$. It is assumed to be higher than the highest temperature (600 K) for which measurements were made (see Ref. 15).

three temperature regimes in the semiconducting region, with activation energies E_1 , E_2 , and E_3 (see Fig. 2). These activation energies generally increase with temperature and decrease with selenium concentration. For example, $E_1 = 4$ meV, $E_2 = 78$ meV, and $E_3 = 240$ meV for the $\text{NiS}_{1.9}\text{Se}_{0.1}$ sample (see Fig. 2). These activation energies are used to fit the exponential dependencies of the electrical conductivity in the semiconducting region. All three temperature regimes have been also observed for the $\text{Ni}_{1-y}\text{Co}_y\text{S}_2$ system in the dilute limit ($y \leq 0.05$).¹¹ The main difference between the two systems is that in the $\text{Ni}_{1-y}\text{Co}_y\text{S}_2$ system, E_3 decreases with increasing y for $0.05 \leq y \leq 0.12$.^{11,12} We have not observed any such decrease of E_3 in the $\text{NiS}_{2-x}\text{Se}_x$ system.

In the $\text{NiS}_{2-x}\text{Se}_x$ system, the substitution of Se for S does not change the carrier concentration. In nominally pure NiS_2 , the electrical conductivity is dominated by a small number of holes in the valence band,¹¹ arising from nickel vacancies.²⁰ We expect that similar defects are responsible for the free carriers in the $\text{NiS}_{2-x}\text{Se}_x$ system. Since the thermopower is positive at low temperatures for $x < 0.52$, the free carriers are predominantly holes. These holes form small polarons in the lower of the correlation-split bands. For $kT \ll U$, the electrical conduction is due almost entirely to the thermally activated hopping of these small polarons in the valence band. At higher temperatures ($kT \approx 0.1 U$) the number of carriers increases roughly as $\exp(-U/2kT)$ due to thermal depopulation of the valence band. In the semiconducting region, the conductivity and thermopower are given by^{12,21,22}

$$\sigma = \frac{4n_0(T)e\mu_0 R \exp(-\beta E_H) \exp\{\beta U\} [1 + R^2 \exp\{\beta U\}]}{[1 + 2R \exp\{\beta U\} + R^2 \exp\{\beta U\}]^2}, \quad (1)$$

$$S = \frac{-k}{e} \left(\frac{\beta U}{1 + R^2 \exp\{\beta U\}} + \ln R \right) - \frac{k}{e} \eta, \quad (2)$$

where $U = U_0 - \gamma kT$ and U_0 is the zero-temperature band gap, γ the temperature coefficient of band collapse, μ_0 the infinite temperature mobility, E_H the hopping activation energy, η an entropy term,²³ and

$$R = e^{\beta(E_F - U)} = \frac{\hat{y} + [\hat{y}^2 + (1 - \hat{y}^2)e^{-\beta U}]^{1/2}}{1 - \hat{y}}, \quad (3)$$

where \hat{y} is the free-hole concentration resulting from nonstoichiometry.^{12,24} Thus, the adjustable parameters in this model are U_0 , γ , μ_0 , E_H , η , and \hat{y} . The present curve-fitting procedure is similar to that recently reported for the $\text{Ni}_{1-y}\text{Co}_y\text{S}_2$ system,^{11,12} the main difference being that \hat{y} , the effective hole concentration in the $\text{NiS}_{2-x}\text{Se}_x$ system,

is a small undetermined parameter of the order of magnitude of the free-hole concentration found in nominally pure NiS_2 ($y < 0.01$).²⁰ The parameter \hat{y} thus plays a similar role to the doping concentration y in the $\text{Ni}_{1-y}\text{Co}_y\text{S}_2$ system, where the holes are introduced systematically via cobalt doping.^{11,12}

The following procedure is used to obtain the parameters that enter Eqs. (1) and (2), thereby yielding the theoretical curves shown in Figs. (1) and (5):

(a) The hopping energy E_H is chosen to be the slope of $\ln \sigma$ vs $1/T$ at low temperatures in the regime where the activation energy is E_2 (see Fig. 2).

(b) U_0 is determined by the slope of $\ln \sigma$ vs $1/T$ in the regime where the activation energy is E_3 .

(c) An estimate for γ is obtained from the thermopower crossover temperature T_0 as given by Bari.²¹

(d) An estimate for μ_0 is obtained by the parameters E_H , U_0 , and γ determined above, together with an estimate for \hat{y} taken from Refs. 12 and 20 to fit Eq. (1) at one intermediate temperature. $N_0(T)$ is taken as the nickel concentration $\approx 5.4 \times 10^{21} \text{ cm}^{-3}$. Suitable adjustments of the parameters are then made to obtain the best fit for σ (see Fig. 1).

The parameters found for σ are then used to make an estimate of the thermopower, neglecting for the moment the entropy term $-(k/e)\eta$. The constant entropy term is then chosen to shift the calculated curve so that agreement with the experimental curves is obtained.

Table III and Fig. 7 give the variation of the parameters with selenium concentration x . It is clear that the parameters U_0 and E_H vary monotonically and relatively slowly with x and approach those previously used for pure NiS_2 .¹¹ (The other parameters γ , μ_0 , and \hat{y} are relatively insensitive

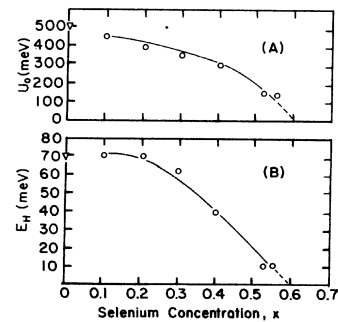


FIG. 7. Plot of U_0 (A) and E_H (B) (meV) vs selenium concentration x . Both energies approach zero at $x \approx 0.6$, where the semiconductor-to-metal transition occurs. The values of the parameters for NiS_2 obtained from Ref. 11 are shown by ∇ .

TABLE III. Values for various parameters for semiconducting $\text{NiS}_{2-x}\text{Se}_x$, $0.1 \leq x \leq 0.55$.

Selenium concentration x	U_0^a (meV)	E_H^b (meV)	γ^c	μ_0^d ($\text{cm}^2/\text{V sec}$)	η^e	\hat{y}^f
0.1	450	70	4.5	1.8	0.29	0.007
0.2	400	70	4.5	2.0	0.29	0.008
0.3	350	70	4.0	1.8	0.32	0.009
0.4	250	40	3.5	2.0	0.29	0.009
0.52	160	10	3.0	1.3	0.29	0.01
0.55	160	10	3.0	1.4	0.29	0.01

^a U_0 is the zero-temperature band gap.

^b E_H is the hopping activation energy.

^c γ is the temperature coefficient for band-gap collapse.

^d μ_0 is the infinite temperature mobility.

^e η is an entropy parameter.

^f \hat{y} is the effective hole concentration.

to x .) This gives us some confidence that the model makes physical sense. It can be seen from Figs. 1 and 5 that the model does provide a good fit to the electrical conductivity and thermopower data for the $\text{NiS}_{2-x}\text{Se}_x$ system in the semiconducting region. The maximum carrier mobilities $\mu = \mu_0 e^{-E_H/kT}$ at 600 K are in the range $0.4 < \mu < 1.1 \text{ cm}^2/\text{V-sec}$ for all x . These values are sufficiently small so that small-polaron transport is likely.

At low temperatures, the assumption $\Delta \ll kT$ is invalid so that the model does not apply. This explains why the data in Figs. 1 and 5 deviate from the theoretical predictions in the low-temperature regime. As the selenium concentration increases, the bandwidth increases, and we should expect an increase in the critical temperature below which the model becomes inadequate. For $x \leq 4$, discrepancies between theory and experiment appear below about 120 K, whereas near $x = 0.6$ the model is inapplicable below 160 K.

To summarize, the main characteristics of our model for the $\text{NiS}_{2-x}\text{Se}_x$ system are: (a) The e_g band in NiS_2 is Hubbard-split into two bands separated by U_0 at $T = 0$ K. (b) For pure NiS_2 the lower band is filled and the upper band is empty so that NiS_2 is a semiconductor. (c) However, nonstoichiometry in NiS_2 leads to a small hole concentration ($< 1\%$) caused mainly by nickel vacancies, in agreement with the vacancy concentration measured by Krill *et al.*²⁰ Addition of selenium leads to an increase in the concentration of nickel vacancies. (d) The temperature dependence of the energy gap is taken to be $U(T) = U_0 - \gamma kT$.¹⁹ (e) The bandwidth Δ is assumed to be small compared to the band gap U_0 (i.e., $\Delta \ll U_0$); this approximation defines our use of the term narrow band. In the $\text{NiS}_{2-x}\text{Se}_x$ system, Δ is likely to be

larger than in pure NiS_2 since substitution of Se for S results in a broadening of the bands.

B. Semiconductor-to-metal transition

For $0.4 < x < 0.55$, the samples appear to undergo a transition to a metallic state at low temperature. This is surprising in view of the fact that the system remains semiconducting at high temperatures even after the correlation splitting of the bands vanishes.¹¹ However, as Holstein has shown, at very low temperatures a small-polaron band should form,¹⁴ in which conduction is bandlike. However, the bandwidth exponentially decreases with increasing temperature until it becomes smaller than the uncertainty in energy due to the finite lifetime of the band states. Above this temperature, conduction occurs predominantly via thermally activated hopping of small polarons. Thus, we should expect a region of exponentially decreasing conductivity at very low temperature followed by a region of exponentially increasing conductivity at higher temperature. The plot of conductivity as a function of temperature shown in Fig. 8 shows essentially the behavior predicted by Holstein¹⁴ with polaron-band formation dominating below $T = 100$ K. In a somewhat more accurate calculation by Lang and Firsov,²⁵ the transition temperature between the two regimes was found to increase with increasing bandwidth. Figure 8 shows that the transition temperature increases from about 70 K for $x = 0.47$ to about 120 K for $x = 0.55$. Since the bandwidth is increasing with x , this is in agreement with the results of Lang and Firsov.^{13,25} For $x < 0.4$, the polaron-band regime moves to sufficiently low temperatures so that it has not yet been observed. This is presumably

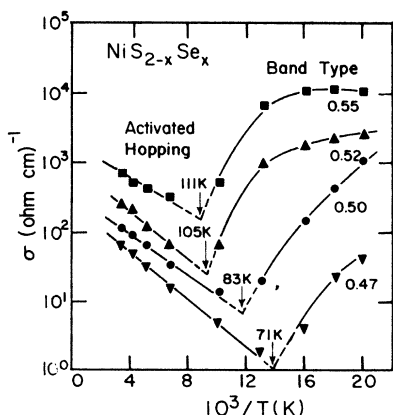


FIG. 8. Conductivity versus inverse temperature $10^3/T$ for $\text{NiS}_{2-x}\text{Se}_x$ showing polaron-band behavior at low temperatures. The conductivity data for $x=0.55$ and 0.52 are from our data and the data for $x=0.50$ and 0.47 are from Ref. 13.

also the case for the $\text{Ni}_{1-y}\text{Co}_y\text{S}_2$ system for $y < 0.12$.^{11,12} The exponential decrease of bandwidths with increasing temperature taken together with the band narrowing effect at zero temperature due to small-polaron formation¹⁴ explains why the narrow bandwidth approximation¹⁴ is valid for materials such as NiS_2 and NiO .²⁶ A rough estimate of the band narrowing can be made by writing the polaron bonding energy as $E_b \approx 2E_H$ and taking $\hbar\omega_0$ a typical lattice mode energy as $\hbar\omega_0 \approx \frac{1}{2}k\theta_D$, where θ_D is the Debye temperature. For NiS_2 , $k\theta_D \sim \frac{1}{40}$, leading to a band narrowing factor $\exp(-E_b/\hbar\omega_0) \sim 10^{-11}$. We would also like to point out that the theories by both Holstein¹⁴ and Lang and Firsov²⁵ are somewhat idealized. They assume

perfect crystals and their calculations are for a nonadiabatic regime.

CONCLUSIONS

We have measured the electrical conductivity, Hall effect, and thermoelectric power as a function of temperature for single crystals of the $\text{NiS}_{2-x}\text{Se}_x$ system ($0 \leq x \leq 1.5$). All results are consistent with the recent conclusions of Mabatah *et al.*⁷ that NiS_2 is a Mott insulator because of the correlation splitting of the Ni $3d e_g$ band. In all real samples, Ni vacancies and/or trace impurities lead to small hole concentrations. As Se replaces S, the bandwidth increases. For $x < 0.55$, transport at all temperatures is due to thermally activated hopping of small polarons. For $0.45 < x < 0.6$, conduction occurs predominantly in a small-polaron band below about 100 K, as predicted by Holstein¹⁴ and others.²⁵ For $x > 0.6$, the system is metallic at all temperatures.

ACKNOWLEDGMENTS

We gratefully acknowledge help with the experimental work from Dr. A. K. Mabatah of the Physics Department, University of Benin, Benin, Nigeria. We also wish to thank Dr. E. Yoffa of IBM and Dr. P. Eklund, Department of Physics, University of Kentucky, Lexington, Kentucky for valuable discussions. We wish to thank Dr. J. Kalnajs, Dr. D. Gabbe, and Dr. A. Linz of the M.I.T. Center for Materials Science and Engineering Crystal Physics Laboratory for help with sample preparation. We also acknowledge the technical assistance of Mr. A. Colozzi. This work was supported by the NSF-MRL program Grant No. DMR 76-80895.

*Department of Physics.

†Department of Electrical Engineering and Computer Science.

¹T. A. Bither, R. J. Bouchard, W. H. Cloud, P. C. Donohue, and W. J. Siemons, *Inorg. Chem.* **7**, 2208 (1968).

²S. Ogawa, S. Waki, and T. Teranishi, *Int. J. Mag.* **5**, 349 (1974).

³J. A. Wilson and A. D. Yoffe, *Advan. Phys.* **18**, 193 (1969).

⁴M. A. Khan, *J. Phys. C* **9**, 81 (1976).

⁵E. K. Li, K. H. Johnson, D. E. Eastman, and J. L. Freeouf, *Phys. Rev. Lett.* **32**, 470 (1974).

⁶A. Ohsawa, H. Yamamoto, and H. Watanabe, *J. Phys. Soc. Jpn.* **37**, 568 (1974).

⁷A. K. Mabatah, E. J. Yoffa, P. C. Eklund, M. S. Dresselhaus, and D. Adler, *Phys. Rev. Lett.* **39**, 494 (1977).

⁸J. M. Hastings and L. M. Corliss, *IBM J. Res. Dev.* **14**, 227 (1970).

⁹N. Mori, T. Mitsui, and S. Yomo, in *Proceedings of*

the 4th International Conference on High Pressure, Kyoto, 1974 (unpublished), p. 295.

¹⁰J. A. Wilson and G. D. Pitt, *Philos. Mag.* **23**, 1297 (1971).

¹¹A. K. Mabatah, E. J. Yoffa, P. C. Eklund, M. S. Dresselhaus, and D. Adler, *Phys. Rev. B* **21**, 1676 (1980).

¹²E. J. Yoffa and D. Adler, *Phys. Rev. B* **12**, 2260 (1975).

¹³R. J. Bouchard, J. L. Gillson, and H. S. Jarrett, *Mat. Res. Bull.* **8**, 489 (1973).

¹⁴T. Holstein, *Ann. Phys. (N. Y.)* **8**, 325 (1959).

¹⁵P. Kwizera, M. Sc. thesis, M. I. T., 1978 (unpublished).

¹⁶D. D. Klemm, *Neues Jahrb. Mineral, Monatshe.* **1962**, 32 (1962).

¹⁷L. J. van der Pauw, *Philips Res. Rep.* **13**, 1 (1958).

¹⁸P. C. Eklund and A. K. Mabatah, *Rev. Sci. Instrum.* **48**, 775 (1977).

¹⁹R. L. Kautz, M. S. Dresselhaus, D. Adler, and A. Linz, in *Proceedings of the 11th International Conference on the Physics of Semiconductors* (Polish

Scientific Publishers, Warsaw, 1972), p. 807.

²⁰G. Krill, M. F. Lapierre, F. Gautier, C. Robert, G. Czjzek, J. Fink, and H. Schmidt, *J. Phys. C* **9**, 761 (1976).

²¹R. A. Bari, *Phys. Rev. B* **10**, 1560 (1974).

²²G. Beni, *Phys. Rev. B* **10**, 2186 (1974).

²³R. R. Heikes, *Thermoelectricity*, edited by R. R. Heikes and W. U. Ure (Interscience, New York, 1961),

Chap. IV.

²⁴A. K. Mabatah, Ph.D. thesis, M.I.T., 1977 (unpublished).

²⁵I. G. Lang and A. Yu Firsov, *Fiz. Tver. Tela (Leningrad)* **5**, 2799 (1963). [*Sov. Phy. Solid State* **5**, 2049 (1964)].

²⁶D. Adler and J. Feinleib, *Phys. Rev. B* **2**, 3112 (1970).